

# Proceedings of the Institution of Mechanical Engineers, Part I: Journal of Systems and Control Engineering

<http://pii.sagepub.com/>

---

## **Adaptive control of Hammerstein systems with unknown Prandtl–Ishlinskii hysteresis**

Mohammad Al Janaideh and Dennis S Bernstein

*Proceedings of the Institution of Mechanical Engineers, Part I: Journal of Systems and Control Engineering* published online 9 October 2014

DOI: 10.1177/0959651814551660

The online version of this article can be found at:

<http://pii.sagepub.com/content/early/2014/10/08/0959651814551660>

---

Published by:



<http://www.sagepublications.com>

On behalf of:



[Institution of Mechanical Engineers](http://www.institutionofmechanicalengineers.org)

**Additional services and information for *Proceedings of the Institution of Mechanical Engineers, Part I: Journal of Systems and Control Engineering* can be found at:**

**Email Alerts:** <http://pii.sagepub.com/cgi/alerts>

**Subscriptions:** <http://pii.sagepub.com/subscriptions>

**Reprints:** <http://www.sagepub.com/journalsReprints.nav>

**Permissions:** <http://www.sagepub.com/journalsPermissions.nav>

**Citations:** <http://pii.sagepub.com/content/early/2014/10/08/0959651814551660.refs.html>

>> [OnlineFirst Version of Record](#) - Oct 9, 2014

[What is This?](#)

# Adaptive control of Hammerstein systems with unknown Prandtl–Ishlinskii hysteresis

Proc IMechE Part I:

*J Systems and Control Engineering*

1–9

© IMechE 2014

Reprints and permissions:

sagepub.co.uk/journalsPermissions.nav

DOI: 10.1177/0959651814551660

pii.sagepub.com



Mohammad Al Janaideh<sup>1</sup> and Dennis S Bernstein<sup>2</sup>

## Abstract

We numerically investigate the sense in which an adaptive control law achieves internal model control of Hammerstein plants with Prandtl–Ishlinskii hysteresis. We apply retrospective cost adaptive control to a command-following problem for uncertain Hammerstein systems with hysteretic input nonlinearities. The only required modeling information of the linear plant is a single Markov parameter. Describing functions are used to determine whether the adaptive controller inverts the plant at the exogenous frequencies.

## Keywords

Actuators, adaptive control systems, automatic control systems, nonlinear control, numerical modelling/simulation

Date received: 8 December 2013; accepted: 7 August 2014

## Introduction

Considerable effort has been devoted to developing methods that enhance the tracking performance of hysteretic systems. These algorithms include inverse-based control methods, model-based control methods, and linear model-free control methods. Inverse-based fixed-gain, robust, and adaptive methods use the inverse of the hysteresis nonlinearity in the feedforward path to compensate for the hysteresis nonlinearity.<sup>1–7</sup> Alternatively, model-based hysteresis techniques employ the hysteresis models to construct controllers that compensate for the actuator hysteresis without the explicit goal of hysteresis inversion. These methods include robust adaptive,<sup>8</sup> energy-based,<sup>9</sup> phase control,<sup>10</sup> and hybrid control systems,<sup>11</sup> which employ a hysteresis model of the actuator for constructing the controller. Finally, linear control methods have been used to compensate for the hysteresis nonlinearity without using a model of the hysteresis. These model-free methods include proportional–integral–derivative (PID) controllers.<sup>12,13</sup>

In this article, we follow the model-free approach by numerically investigating the ability of an adaptive control law to achieve internal model control of Hammerstein plants with unknown input hysteresis. The internal model principle states that a stabilizing control law that achieves asymptotically perfect command-following or disturbance rejection must

“possess” a model of the exogenous signal.<sup>14–17</sup> This principle is the basis of PID control, where the integrator can be viewed as a model of a step command or step disturbance.<sup>18</sup> It is worth noting that, in a classical servo loop, where the objective is command-following, the requirement for an internal model in the loop transfer function can be satisfied by the plant itself, but this is not the case for disturbance rejection. For example, asymptotic command-following for a step command with a plant that has a pole at 0 is achieved by any stabilizing controller, although rejection of a step command requires that the controller provide integral action.

In this article, we revisit internal model control within the context of adaptive control of Hammerstein systems. Although we focus on retrospective cost adaptive control (RCAC),<sup>19–25</sup> which requires minimal plant modeling information as well as no knowledge of the command or disturbance amplitude, frequency, or

<sup>1</sup>Department of Mechatronics Engineering, The University of Jordan, Amman, Jordan

<sup>2</sup>Department of Aerospace Engineering, The University of Michigan, Ann Arbor, MI, USA

### Corresponding author:

Mohammad Al Janaideh, Department of Mechatronics Engineering, The University of Jordan, 11942 Amman, Jordan.

Email: aljanaideh@gmail.com

phase shift, the methodology that we use to assess the controller action can be applied to any control law that achieves internal stability along with either command-following or disturbance rejection. Furthermore, although we focus on discrete-time control of discrete-time (possibly sampled-data) plants, the ideas are applicable to continuous-time systems.

Of special interest is the operation of the control law in terms of phase compensation. Since asymptotically perfect command-following requires that the plant output match the phase and amplitude of the command, the plant input must also be a sinusoid whose amplitude and phase are consistent with the magnitude and phase shift of the plant at the command frequency. However, the phase of the control input cannot be determined in terms of the phase shift of the controller due to the fact that an internal model controller has a phase discontinuity at the command frequency. Instead, the frequency response of the transfer function from the command to the plant input is used to determine whether the control law inverts the plant at the command frequency.

The numerical investigation in this article is intended to motivate future theoretical studies of adaptive control of hysteretic Hammerstein systems with harmonic commands and disturbances. In particular, we use the classical technique of describing functions to determine whether RCAC provides correct phase compensation in the presence of an unknown hysteretic input nonlinearity. The Prandtl–Ishlinskii hysteresis model is used to represent the input nonlinearity.

This article shows that the classical technique of describing functions can shed light on the performance of adaptive control laws. We stress that the diagnostics that we use are not confined to RCAC, but can be used to investigate the asymptotic properties of any control law that is applicable to either harmonic command-following (possibly model reference adaptive control (MRAC)) or harmonic disturbance rejection. The objective is to show that RCAC can achieve internal model control of Hammerstein systems with an unknown Prandtl–Ishlinskii input hysteresis. The describing function was used to show that RCAC inverts the Hammerstein system at the command frequency of the harmonic command input.

### Background

We begin with nonadaptive control for a servo loop with harmonic commands. For a single-input single-output (SISO) system linear time-invariant (LTI) plant, we choose an internal model control law under the assumption that the command frequency is known. Consider the linear system

$$x(k + 1) = Ax(k) + Bu(k) \tag{1}$$

$$y(k) = Cx(k) \tag{2}$$

$$e(k) = y(k) - r(k) \tag{3}$$

where  $x(k) \in \mathbb{R}^n$  is the state,  $y(k) \in \mathbb{R}$  is the measured output available to the controller,  $e(k) \in \mathbb{R}$  is the command-following error,  $u(k) \in \mathbb{R}^1$  is the control,  $r(k) \in \mathbb{R}$  is the command,  $A$  is the state matrix,  $B$  is the input matrix, and  $C$  is the output matrix.

The goal is to determine  $u$  that stabilizes the closed-loop system and makes tracking error  $e$  small. The closed-loop system presented in Figure 1 can be represented by the cascaded system in Figure 2, where

$$G_{ur}(\mathbf{q}) = \frac{G_c(\mathbf{q})}{1 + G_c(\mathbf{q})G(\mathbf{q})} \tag{4}$$

where  $\mathbf{q}$  is the forward shift operator.

Suppose that the command is the harmonic signal  $r(k) = \text{Re}\{A_r e^{j\Omega k}\}$ , where  $A_r$  is a complex number and  $\Omega$  is the command frequency with units rad/sample. If  $G_{ur}$  is asymptotically stable and  $u$  is also harmonic, then

$$u(k) = \text{Re}\left\{A_r |G_{ur}(e^{j\Omega})| e^{j(\Omega k + \angle G_{ur}(e^{j\Omega}))}\right\} \tag{5}$$

where  $|G_{ur}(e^{j\Omega})|$  and  $\angle G_{ur}(e^{j\Omega})$  are the magnitude and phase of  $G_{ur}$  at the frequency  $\Omega$ , respectively. Then, the harmonic steady-state response is given by

$$y(k) = \text{Re}\left\{A_r |G_{ur}(e^{j\Omega})| |G(e^{j\Omega})| e^{j(\Omega k + \angle G_{ur}(e^{j\Omega}) + \angle G(e^{j\Omega}))}\right\} \tag{6}$$

The command-following error  $e$  is given by

$$e(k) = \text{Re}\{A_r e^{j\Omega k}\} - \text{Re}\left\{A_r |G_{ur}(e^{j\Omega})| |G(e^{j\Omega})| e^{j(\Omega k + \angle G_{ur}(e^{j\Omega}) + \angle G(e^{j\Omega}))}\right\} \tag{7}$$

Therefore,  $e(k) = 0$  if and only if the magnitude and phase of  $G_{ur}(e^{j\Omega})$  satisfy

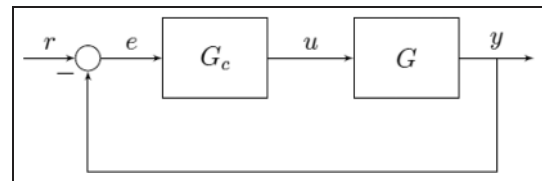


Figure 1. Command-following problem for the linear plant  $G$  with the controller  $G_c$ .

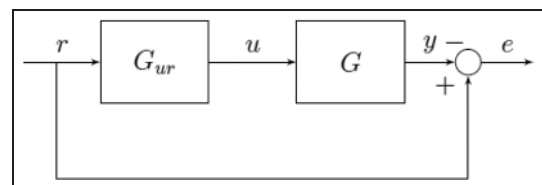
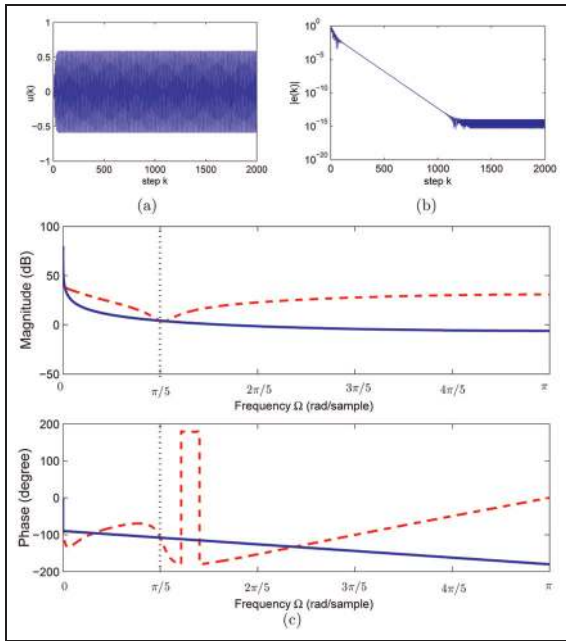
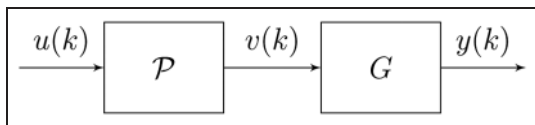


Figure 2. Representation of the command-following problem as a cascaded system.



**Figure 3.** Example 2.1 shows (a) the control input  $u(k)$ , (b) the command-following error  $e(k)$ , and (c) the frequency response of  $G$  (solid line) and  $1/G_{ur}$  (dashed line). Note that the magnitude and phase of  $G$  and  $1/G_{ur}$  coincide at the command frequency  $\Omega = \pi/5$  rad/sample.



**Figure 4.** Hammerstein system with Prandtl-Ishlinskii hysteresis  $\mathcal{P}$ .

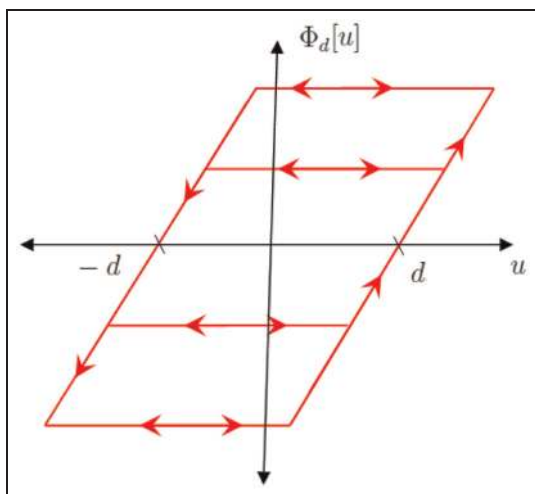


**Figure 5.** The play operator with threshold  $d$ .

$$|G_{ur}(e^{j\Omega})| = \frac{1}{|G(e^{j\Omega})|} \tag{8}$$

$$\angle G_{ur}(e^{j\Omega}) = -\angle G(e^{j\Omega}) \tag{9}$$

**Example 2.1**

Let  $r(k) = \sin(\pi/5(k))$  and consider the Lyapunov-stable plant  $G(z) = 1/(z - 1)$  and the stabilizing internal model controller  $G_c(z) = 0.01846(z/z^2 - 1.902z + 1)(z - 1.1/(z - 0.1))^2$ . Figure 3 shows that the error approaches 0 and that  $G_{ur}$  inverts the plant  $G$  at the command frequency  $\Omega$ .

Figure 3 shows that  $G_{ur}$  stabilizes the closed-loop system and decreases the command-following error  $e$  for the harmonic command  $r$ . Furthermore, the  $G_{ur}$  inverts the phase and magnitude of the Lyapunov-stable plant  $G(z) = 1/(z - 1)$  at the command frequency  $\Omega = \pi/5$  rad/sample.

**Hammerstein system with input hysteresis**

We consider the Hammerstein system shown in Figure 4, where  $\mathcal{P}$  is a Prandtl-Ishlinskii hysteresis model.

**Prandtl-Ishlinskii hysteresis**

The Prandtl-Ishlinskii hysteresis model is used to represent hysteresis in piezoceramic and magnetostrictive actuators.<sup>2-4, 15</sup> This model is based on a linear combination of play operators. For an input  $u(k)$ , the output  $v(k)$  of the Prandtl-Ishlinskii model is represented by

$$v(k) = \mathcal{P}[u](k) \triangleq \sum_{i=1}^n \kappa_i \Phi_{d_i}[u](k) \tag{10}$$

where  $\kappa_1, \dots, \kappa_n$  are positive weights and the backlash operator with threshold  $d_i$  is defined by

$$\Phi_{d_i}[u](k) \triangleq \begin{cases} u(k) - d_i, & \text{if } u(k) > d_i \text{ and } u(k) > u(k-1) \\ u(k) + d_i, & \text{if } u(k) < d_i \text{ and } u(k) < u(k-1) \\ \Phi_{d_i}[u](k-1), & \text{otherwise} \end{cases} \tag{11}$$

with the initial condition

$$\Phi_{d_i}[u](0) = \begin{cases} u(0) - d_i, & \text{if } u(0) > d_i \\ u(0) + d_i, & \text{if } u(0) < d_i \\ 0, & \text{otherwise} \end{cases} \tag{12}$$

The backlash operator is shown in Figure 5. Since the backlash operator (11) is rate-independent, it follows that the Prandtl-Ishlinskii model is also rate-independent.

**Problem reformulation**

In place of equation (1), consider the Hammerstein system consisting of equations (2) and (3) and

$$x(k+1) = Ax(k) + Bv(k) \quad (13)$$

$$v(k) = \mathcal{P}[u](k) \quad (14)$$

$$y(k) = Cx(k) \quad (15)$$

where  $\mathcal{P}$  is the Prandtl–Ishlinskii hysteresis model. The goal is to determine  $u$  that makes  $e$  small.

### A describing function for the Prandtl–Ishlinskii hysteresis model

Let  $u(k) = \text{Re}\{A_u e^{j\Omega k}\}$ , where  $A_u$  is a complex number. For  $i = 1, \dots, n$ , let

$$v_i(k) = \Phi_{d_i}[u](k) \quad (16)$$

For  $|A_u| > d_i$

$$v_i(k) \cong \text{Re}\{|A_u| F_i(|A_u|) e^{j(\Omega k + \angle F_i(|A_u|))}\} \quad (17)$$

where the amplitude  $|F_i(|A_u|)|$  and phase  $\angle F_i(|A_u|)$  of the describing function of the backlash operator are given by<sup>26</sup>

$$|F_i(|A_u|)| = \frac{1}{|A_u|} \sqrt{a_i^2 + b_i^2} \quad (18)$$

$$\angle F_i(|A_u|) = \tan^{-1} \frac{a_i}{b_i} \quad (19)$$

where

$$a_i \triangleq \frac{2d_i}{\pi} (\eta_{\rho_i} - 1) \quad (20)$$

$$b_i \triangleq \frac{|A_u|}{\pi} \left( \frac{\pi}{2} - \sin^{-1} \eta_{\rho_i} - \eta_{\rho_i} \sqrt{1 - \eta_{\rho_i}^2} \right) \quad (21)$$

where

$$\eta_{\rho_i} \triangleq \frac{2d_i}{|A_u|} - 1$$

The describing function of the Prandtl–Ishlinskii hysteresis model is given approximately by

$$H(\Omega, |A_u|) \triangleq \sum_{i=1}^n \kappa_i \text{Re}\{|F_i(|A_u|)| e^{j(\angle F_i(|A_u|))}\} \quad (22)$$

Then, the output of the Prandtl–Ishlinskii hysteresis model is thus given approximately by

$$v(k) \triangleq \sum_{i=1}^n \kappa_i \text{Re}\{A_u |F_i(|A_u|)| e^{j(\Omega k + \angle F_i(|A_u|))}\} \quad (23)$$

Consequently, ignoring transient effects, the output of equations (1) and (2) is given approximately by

$$y(k) \cong \sum_{i=1}^n \text{Re}\{A_r |G(e^{j\Omega})| F_i(|A_r|) e^{j(\Omega k + \angle F_i(|A_r|) + \angle G(e^{j\Omega}))}\} \quad (24)$$

**Example 3.1.** We consider the command  $u(k) = \sin(\Omega k)$ , where  $\Omega = \pi/5$  rad/sample, the Prandtl–Ishlinskii model  $\mathcal{P}$  with  $n = 3$ ,  $d_1 = 0.1$ ,  $d_2 = 0.2$ ,  $d_3 = 0.3$ ,

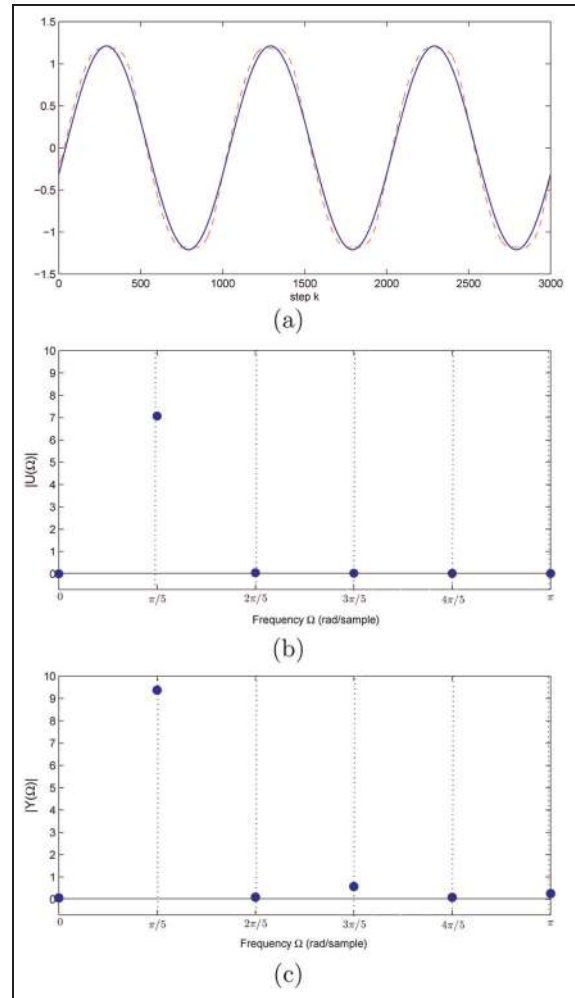


**Figure 6.** (a) The output (23) of the describing function (solid line) and the Prandtl–Ishlinskii model (10) (dashed line), (b) the magnitude of the discrete Fourier transform  $|U(\Omega)|$  of the command signal, and (c) the magnitude of the discrete Fourier transform  $|Y(\Omega)|$  of the output of the Prandtl–Ishlinskii model.

$\kappa_1 = 0.6$ ,  $\kappa_2 = 0.5$ ,  $\kappa_3 = 0.4$ . Figure 6(a) compares the output of the Prandtl–Ishlinskii model and the describing function output (23). Figure 6(b) shows the magnitude of the discrete Fourier transform  $|U(\Omega)|$  of the command signal. As shown in Figure 6(b), the magnitude of the discrete Fourier transform  $|Y(\Omega)|$  of the output of the Prandtl–Ishlinskii model indicates the presence of harmonics at only odd multiples of the command frequency  $\Omega$ . The presence of these harmonics is consistent with the fact that the hysteresis map of the Prandtl–Ishlinskii model is an odd set-valued map.

### Adaptive control of Hammerstein systems with Prandtl–Ishlinskii hysteresis

Various techniques have been used to control systems with uncertain input nonlinearities and linear dynamics.<sup>1</sup> In this article, we focus on RCAC. Note that, unlike,<sup>1</sup> RCAC does not attempt to estimate the hysteresis nonlinearity.

For the Hammerstein command-following problem, we assume that  $G$  is unknown except for an estimate of a single nonzero Markov parameter and nonminimum-phase zeros, if any are present. The input hysteresis nonlinearity  $\mathcal{P}$  is also unknown.

**Control law**

In this section, we present the adaptive RCAC controller used to formulate  $G_{ur}$ . Consider the controller of order  $n_c$  given by

$$u(k) = \sum_{i=1}^{n_c} M_i(k)u(k-i) + \sum_{i=1}^{n_c} N_i(k)e(k-i) \quad (25)$$

where for all  $i = 1, \dots, n_c$ ,  $M_i(k) \in \mathbb{R}$  and  $N_i(k) \in \mathbb{R}$ . The control (25) can be expressed as

$$u(k) = \theta(k)\phi(k-1)$$

where

$$\theta(k) \triangleq [M_1(k) \dots M_{n_c}(k) \quad N_1(k) \dots N_{n_c}(k)] \in \mathbb{R}^{1 \times 2n_c}$$

is the matrix of controller coefficients, and the regressor vector  $\phi(k)$  is given by

$$\phi(k-1) \triangleq [u(k-1) \quad \dots \quad u(k-n_c) \quad e(k-1) \dots e(k-n_c)]^T \in \mathbb{R}^{2n_c}$$

The transfer function matrix  $G_{c,k}(\mathbf{q})$  from  $e$  to  $u$  at time step  $k$  can be represented by

$$G_{c,k}(\mathbf{q}) = \frac{N_1(k)\mathbf{q}^{n_c-1} + N_2(k)\mathbf{q}^{n_c-2} + \dots + N_{n_c}(k)}{\mathbf{q}^{n_c} - (M_1(k)\mathbf{q}^{n_c-1} + \dots + M_{n_c-1}(k)\mathbf{q} + M_{n_c}(k))}$$

**RCAC**

For  $i \geq 1$ , define the Markov parameter

$$H_i \triangleq CA^{i-1}B$$

For example

$$H_1 = CB$$

and

$$H_2 = CAB$$

Let  $\ell$  be a positive integer. Then, for all  $k \geq \ell$

$$x(k) = A^\ell x(k-\ell) + \sum_{i=1}^{\ell} A^{i-1}BP(u(k-i)) \quad (26)$$

and thus

$$e(k) = CA^\ell x(k-\ell) - r(k) + \bar{H}\bar{U}(k-1) \quad (27)$$

where

$$\bar{H} \triangleq [H_1 \quad \dots \quad H_\ell] \in \mathbb{R}^{1 \times \ell}$$

and

$$\bar{U}(k-1) \triangleq \begin{bmatrix} \mathcal{P}(u(k-1)) \\ \vdots \\ \mathcal{P}(u(k-\ell)) \end{bmatrix}$$

Next, we rearrange the columns of  $\bar{H}$  and the components of  $\bar{U}(k-1)$  and partition the resulting matrix and vector so that

$$\bar{H}\bar{U}(k-1) = \mathcal{H}'U'(k-1) + \mathcal{H}U(k-1) \quad (28)$$

where  $\mathcal{H}' \in \mathbb{R}^{1 \times (\ell-1)}$ ,  $\mathcal{H} \in \mathbb{R}$ ,  $U'(k-1) \in \mathbb{R}^{\ell-1}$ , and  $U(k-1) \in \mathbb{R}$ . Then, we can rewrite equation (27) as

$$e(k) = \mathcal{S}(k) + \mathcal{H}U(k-1) \quad (29)$$

where

$$\mathcal{S}(k) \triangleq CA^\ell x(k-\ell) - r(k) + \mathcal{H}'U'(k-1) \quad (30)$$

Next, we define the retrospective performance

$$\hat{e}(k) = e(k) - \mathcal{H}U(k-1) + \mathcal{H}\hat{U}(k-1) \quad (31)$$

Finally, we define the retrospective cost function

$$J(\hat{U}(k-1), k) \triangleq \hat{e}^2(k) \quad (32)$$

The goal is to determine refined controls  $\hat{U}(k-1)$  that would have provided better performance than the controls  $U(k)$  that were applied to the system. The refined control values  $\hat{U}(k-1)$  are subsequently used to update the controller. Next, to ensure that equation (32) has a global minimizer, we consider the regularized cost

$$\bar{J}(\hat{U}(k-1), k) \triangleq \hat{e}^2(k) + \eta(k)\hat{U}^T(k-1)\hat{U}(k-1) \quad (33)$$

where  $\eta(k) \geq 0$ . Substituting equations (31) into (33) yields

$$\begin{aligned} \bar{J}(\hat{U}(k-1), k) &= \hat{U}(k-1)^T \mathcal{A}(k)\hat{U}(k-1) \\ &\quad + \mathcal{B}(k)\hat{U}(k-1) + \mathcal{C}(k) \end{aligned}$$

where

$$\begin{aligned} \mathcal{A}(k) &\triangleq \mathcal{H}^T \mathcal{H} + \eta(k)I_{\ell} \\ \mathcal{B}(k) &\triangleq 2\mathcal{H}^T[e(k) - \mathcal{H}U(k-1)] \\ \mathcal{C}(k) &\triangleq \hat{e}^2(k) - 2e(k)\mathcal{H}U(k-1) + U^T(k-1)\mathcal{H}^T\mathcal{H}U(k-1) \end{aligned}$$

If either  $\mathcal{H}$  has full column rank or  $\eta(k) > 0$ , then  $\mathcal{A}(k)$  is positive definite. In this case,  $\bar{J}(\hat{U}(k-1), k)$  has the unique global minimizer

$$\hat{U}(k-1) = -\frac{1}{2}\mathcal{A}^{-1}(k)\mathcal{B}(k) \quad (34)$$

Define the cumulative cost function

$$J_R(\theta, k) \triangleq \sum_{i=2}^k \lambda^{k-i} \|\phi^T(i-2)\theta^T(k) - \hat{U}^T(i-1)\|^2 + \lambda^k (\theta(k) - \theta_0) P_0^{-1} (\theta(k) - \theta_0)^T, \tag{35}$$

where  $\|\cdot\|$  is the Euclidean norm, and  $\lambda \in (0,1]$  is the forgetting factor. Minimizing (1) yields

$$\theta^T(k) = \theta^T(k-1) + P(k-1)\phi(k-2) \cdot [\phi^T(k-1)P(k-1)\phi(k-2) + \lambda]^{-1} \cdot [\phi^T(k-2)\theta^T(k-1) - \hat{U}^T(k-1)] \tag{36}$$

The error covariance is updated by

$$P(k) = \lambda^{-1} P(k-1) - \lambda^{-1} P(k-1)\phi(k-2) \cdot [\phi^T(k-2)P(k-1)\phi(k-1) + \lambda]^{-1} \cdot \phi^T(k-2)P(k-1)$$

We initialize the error covariance matrix as  $P(0) = \alpha I_{2n_c}$ , where  $\alpha > 0$ .

### Numerical examples

In this section, we present simulation results for adaptive control of the Hammerstein system presented in Figure 4. The objective is to determine whether RCAC can achieve internal model control in the presence of the unknown input hysteresis nonlinearity.

#### The Prandtl–Ishlinskii hysteresis model

In this section, we consider the Prandtl–Ishlinskii hysteresis nonlinearity. To investigate this question, we examine the magnitude and phase of

$$\tilde{G}_{ur}(e^{j\Omega}) \triangleq \frac{G_{c,2000}(e^{j\Omega})}{1 + H(\Omega, |A_u|)G(e^{j\Omega})G_{c,2000}(e^{j\Omega})} \tag{38}$$

The magnitude  $|\tilde{G}_{ur}(e^{j\Omega})|$  reveals whether the controller  $G_{c,2000}(e^{j\Omega})$  provides high magnitude at the command frequencies and the harmonics introduced by the Hammerstein system in Figure 4. The phase  $\angle \tilde{G}_{ur}(e^{j\Omega})$  shows whether  $G_{c,2000}(e^{j\Omega})$  compensates the phase shift provided by the Hammerstein system presented in Figure 4 at the command frequencies and their harmonics.

**Example 5.1.** Consider the command  $r(k) = \sin(\pi/5(k))$ , the Prandtl–Ishlinskii hysteresis model  $\mathcal{P}$  with  $n = 4$ ,  $d_1 = 0$ ,  $d_2 = 0.1$ ,  $d_3 = 0.2$ ,  $d_4 = 0.3$ ,  $\kappa_1 = 0.8$ ,  $\kappa_2 = 0.6$ ,  $\kappa_3 = 0.4$ ,  $\kappa_4 = 0.3$ , and the asymptotically stable linear plant  $G(z) = (z - 0.5)/((z - 0.8)(z - 0.6))$ . We use RCAC with  $n_c = 14$ ,  $\lambda = 1$ , and  $\alpha = 1$  (Figure 7). Figure 9 shows the closed-loop response. RCAC minimizes the command-following error  $e$  when the input hysteresis nonlinearity shown in Figure 8(b) is considered. Figure 8(e) shows that  $1/\tilde{G}_{ur}$

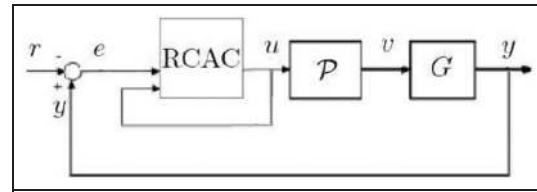


**Figure 7.** Hammerstein command-following problem with the RCAC adaptive controller. The Hammerstein system consists of the input nonlinearity  $\mathcal{P}$  cascaded with the linear plant  $G$ , where  $u$  is the control signal. Measurements of  $y(k)$  are available for feedback; however, measurements of  $v(k) = \mathcal{P}(u(k))$  are not available. RCAC: retrospective cost adaptive control.

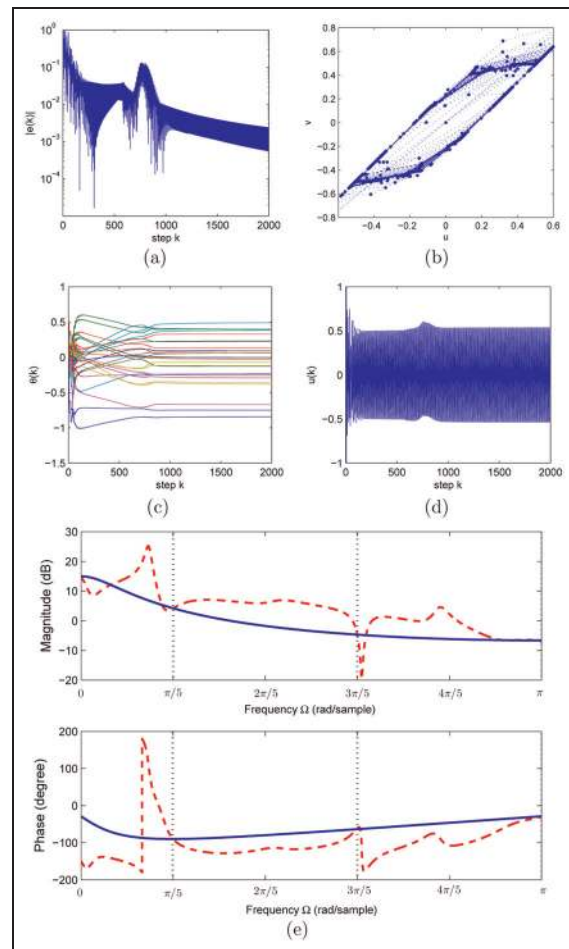


**Figure 8.** Example 5.1 shows (a) the command-following error  $e$  for the asymptotically stable linear plant  $G(z) = (z - 0.5)/((z - 0.8)(z - 0.6))$  with the Prandtl–Ishlinskii model  $\mathcal{P}$  whose input and output are shown in (b) for the closed-loop system with RCAC, (c) the evolution of the controller  $\theta$  and the command-following error  $e$  for the asymptotically stable linear plant  $G(z) = (z - 0.5)/((z - 0.8)(z - 0.6))$ , (d) the control input  $u(k)$ , (e) the frequency response of  $1/\tilde{G}_{ur}$  (dashed line) and  $HG$  (solid line). Note that  $1/\tilde{G}_{ur}$  and  $HG$  coincide at the frequencies  $\pi/5$ ,  $3\pi/5$ , and  $\pi$  rad/sample.

and  $HG$  coincide at the frequencies  $\pi/5$ ,  $3\pi/5$ , and  $\pi$  rad/sample.

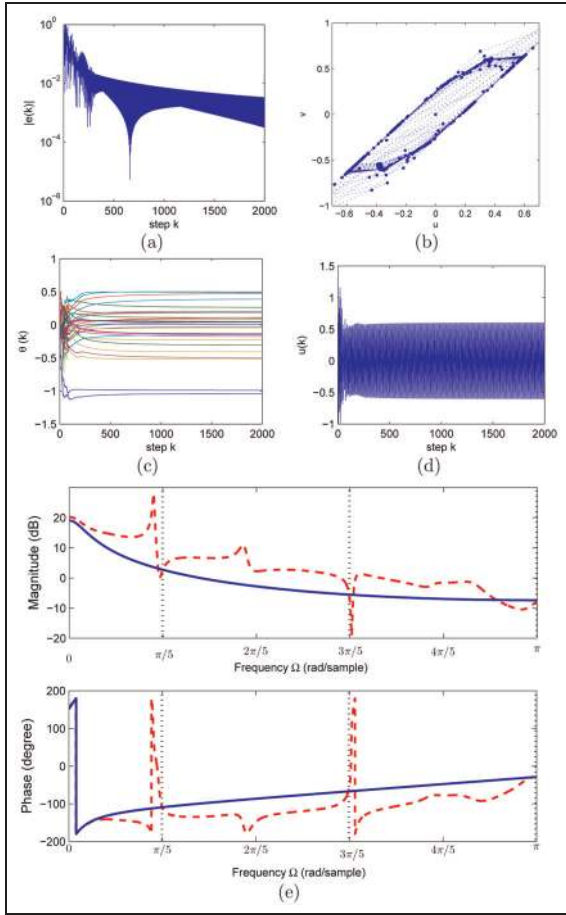


**Figure 9.** Example 5.2 shows (a) the command-following error  $e$  for the unstable linear plant  $G(z) = 1/(z - 1.1)$  with the Prandtl–Ishlinskii model  $\mathcal{P}$ , whose input and output are shown in (b) for the closed-loop system with RCAC; (c) the evolution of the controller  $\theta$  and the command-following error  $e$  for the unstable linear plant  $G(z) = 1/(z - 1.1)$ ; (d) the control input  $u(k)$ ; and (e) the frequency response for  $1/\tilde{G}_{ur}$  (dashed line) and  $HG$  (solid line). Note that  $1/\tilde{G}_{ur}$  and  $HG$  coincide at the frequencies  $\pi/5, 3\pi/5$ , and  $\pi$  rad/sample.

*Example 5.2.* Consider the command  $r(k) = \sin(\pi/5(k))$ , the Prandtl–Ishlinskii model  $\mathcal{P}$  with  $n = 4$ ,  $d_1 = 0, d_2 = 0.1, d_3 = 0.2, d_4 = 0.3, \kappa_1 = 0.8, \kappa_2 = 0.6, \kappa_3 = 0.4, \kappa_4 = 0.3$ , with the unstable plant  $G(z) = 1/(z - 1.1)$ . We use RCAC with  $n_c = 14, \lambda = 1$ , and  $\alpha = 1$  (Figure 7). Figure 9 shows the closed-loop response. Figure 9(e) shows that  $1/\tilde{G}_{ur}$  and  $HG$  coincide at the frequencies  $\pi/5, 3\pi/5$ , and  $\pi$  rad/sample.

Consistent with Example 3.1, the output of the Prandtl–Ishlinskii hysteresis model shows harmonics at odd multiples of the command frequency  $\Omega$ . Examples 5.1 and 5.2 show that  $\tilde{G}_{ur}$  constructed with RCAC inverts the magnitude and phase of the Hammerstein system. That is, the magnitude and phase of  $\tilde{G}_{ur}(e^{j\Omega})$  approximately satisfy

$$|\tilde{G}_{ur}(e^{j\Omega})| = \frac{1}{\sum_{i=0}^n \text{Re}\{A_r|G(e^{j\Omega})|F_i(|A_u|)\}} \quad (39)$$

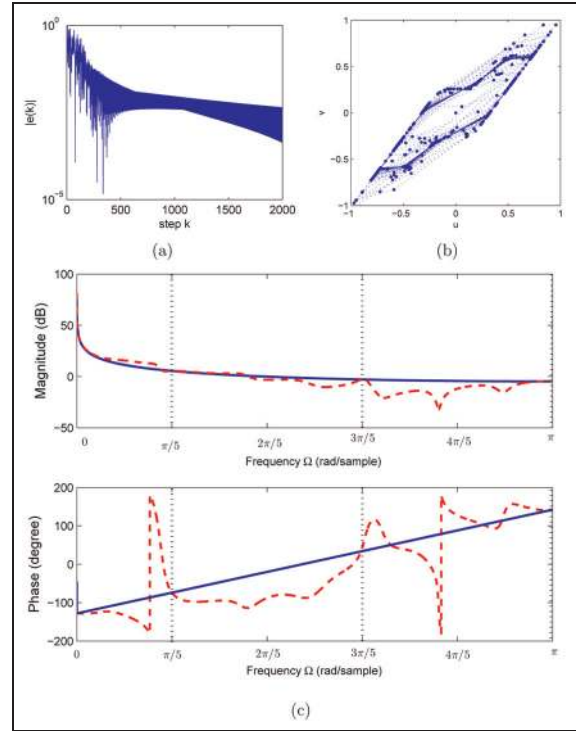


**Figure 10.** Example 5.3 shows (a) the command-following error  $e$  when the Lyapunov-stable plant  $G(z) = 1/(z - 1)$  and the output of the generalized Prandtl–Ishlinskii model  $\mathcal{P}_\gamma$  shown in (b) considered in the closed-loop system with RCAC and (c) the frequency response for  $1/\tilde{G}_{ur}$  (dashed line) and  $H_dG$  (solid line).

$$\angle \tilde{G}_{ur}(e^{j\Omega}) = -\angle G(e^{j\Omega}) - \sum_{i=0}^n \angle F_i(|A_u|) \quad (40)$$

*The generalized Prandtl–Ishlinskii hysteresis model*

In this section, we consider the generalized Prandtl–Ishlinskii model which can characterize non-convex hysteresis loops in smart actuators.<sup>7</sup> The output of this model is expressed as

$$\mathcal{P}_\gamma[u](t) := \sum_{i=0}^n \kappa_i \Phi_{d_i}[\gamma(u)](k) \quad (41)$$

where

$$\gamma(u) = \sum_{i=0}^m g_i \mathcal{D}_{\rho_i}[u](k) \quad (42)$$

$$\mathcal{D}_{\rho_i}[u](k) = \begin{cases} u(k) - \rho_i, & \text{if } u(k) \geq \rho_i \\ 0, & \text{if } -\rho_i \leq u(k) \leq \rho_i \\ u(k) + \rho_i, & \text{if } u(k) \leq -\rho_i \end{cases} \quad (43)$$

where  $g_i$  are positive weights and  $\rho_i$  are positive constants. In this example, we present the describing function for the memoryless function presented in equation (43)



$$H_\gamma(\Omega, |A_u|) = \sum_{i=0}^m \operatorname{Re}\{|A_u| F_{Di}(|A_u|) e^{j\Omega k}\} \quad (44)$$

where  $F_{Di}(|A_u|)$  represents the amplitude of the describing function of the deadzone operator<sup>26</sup>

$$F_{Di}(|A_u|) = \frac{2g_i}{\pi} \left( \frac{\pi}{2} - \sin^{-1} \eta_{\sigma i} - \eta_{\sigma i} \sqrt{1 - \eta_{\sigma i}^2} \right) \quad (45)$$

where

$$\eta_{\sigma i} = \frac{\rho_i}{|A_u|}$$

Let  $H_d(\Omega, |A_u|) = H_\gamma(\Omega, |A_u|)H(\Omega, |A_u|)$ , then

$$\hat{G}_{ur}(e^{j\Omega}) = \frac{G_{c,2000}(e^{j\Omega})}{1 + H_d(\Omega, |A_u|)G(e^{j\Omega})G_{c,2000}(e^{j\Omega})} \quad (46)$$

We examine both the magnitude  $|\hat{G}_{ur}(e^{j\Omega})|$  and the phase  $\angle \hat{G}_{ur}(e^{j\Omega})$  to show whether  $G_{c,2000}(e^{j\Omega})$  compensates the phase shift provided by the Hammerstein system with the generalized Prandtl–Ishlinskii model at the command frequencies and their harmonics.

**Example 5.3.** We consider the command  $r(k) = \sin(\pi/5(k))$ , the generalized Prandtl–Ishlinskii model  $\mathcal{P}_\gamma$  with  $n = 4$ ,  $d_1 = 0$ ,  $d_2 = 0.1$ ,  $d_3 = 0.2$ ,  $d_4 = 0.3$ ,  $\kappa_0 = 0.8$ ,  $\kappa_1 = 0.6$ ,  $\kappa_2 = 0.4$ ,  $\kappa_3 = 0.3$ ,  $m = 1$ ,  $g_0 = g_1 = 0.5$ ,  $\rho_0 = 0.1$ ,  $\rho_1 = 0.2$  with the Lyapunov-stable plant  $G(z) = 1/(z - 1)$ . We use RCAC with  $n_c = 18$ ,  $\lambda = 1$ , and  $\alpha = 9$ . Figure 10 shows stimulation results.

**Example 5.4.** In this example, we consider the piezoceramic actuator described in Shan and Leang.<sup>27</sup> The Prandtl–Ishlinskii hysteresis model  $\mathcal{P}$  and

$$G(s) = \frac{3.391 \times 10^{10}}{s^3 + 3759s^2 + 2.063 \times 10^7s + 7.514 \times 10^{10}} \quad (47)$$

characterize the dynamic behavior of the actuator.<sup>27</sup> For the closed-loop control system, we consider  $n = 8$ ,  $d_1 = 0.0769$ ,  $d_2 = 0.1538$ ,  $d_3 = 0.2307$ ,  $d_4 = 0.3076$ ,  $d_5 = 0.3845$ ,  $d_6 = 0.4614$ ,  $d_7 = 0.5383$ ,  $d_8 = 0.6152$ ,  $\kappa_1 = 3.6590$ ,  $\kappa_2 = 2.8098$ ,  $\kappa_3 = 2.1577$ ,  $\kappa_4 = 1.6569$ ,  $\kappa_5 = 1.2724$ ,  $\kappa_6 = 0.9771$ ,  $\kappa_7 = 0.7503$ ,  $\kappa_8 = 0.5762$ , and

$$\gamma(v) = 0.6081v + 0.0039 \quad (48)$$

We consider the sampling time of  $h = 0.00001$  sec. Then

$$G(z) = \frac{0.256z^2 + 0.02439z + 0.1349}{z^3 - 0.5746z^2 + 0.4949z - 9.137 \times 10^{-17}} \quad (49)$$

We use RCAC with  $n_c = 10$ ,  $\lambda = 1$ , and  $\alpha = 100$ . Figure 10 shows the simulation results.

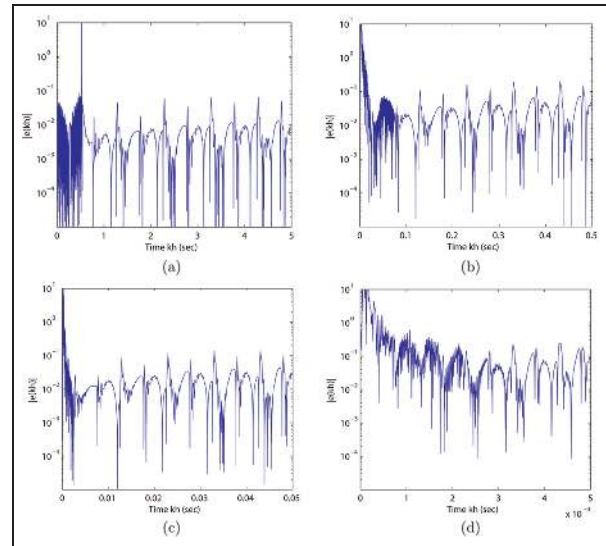


**Figure 11.** Example 5.4 shows the command-following error  $e$  with the command signal  $r(t) = 10 \sin(\omega h k)$  with  $h = 0.00001$  sec: (a)  $\omega = 2\pi$  rad/sample, (b)  $\omega = 20\pi$  rad/sample, (c)  $\omega = 200\pi$  rad/sample, and (d)  $\omega = 2000\pi$  rad/sample.

## Conclusion

The numerical investigation in this article shows that RCAC can achieve internal model control of Hammerstein systems with an unknown Prandtl–Ishlinskii input hysteresis. A describing function was used to show that RCAC inverts the Hammerstein system at the command frequency of the harmonic command input.

Future work will include theoretical studies of adaptive control with harmonic commands for Hammerstein systems and disturbances as well as extension to Preisach model.

## Declaration of conflicting interests

The authors declare that there is no conflict of interest.

## Funding

This research received no specific grant from any funding agency in the public, commercial, or not-for-profit sectors.

## References

1. Tao G and Kokotović P. *Adaptive control of systems with actuator and sensor nonlinearities*. New York: Wiley, 1996.
2. Krejci P, Al Janaideh M and Deasy F. Inversion of hysteresis and creep operators. *Physica B* 2012; 407(8): 1354–1356.
3. Visone C and Sjöström M. Exact invertible hysteresis models based on play operators. *Physica B* 2004; 343(1): 148–152.
4. Kuhnen K. Modeling, identification and compensation of complex hysteretic nonlinearities: a modified Prandtl–Ishlinskii approach. *Eur J Control* 2003; 9(4): 407–418.

5. Esbrook A, Tan X and Khalil H. Control of systems with hysteresis via servocompensation and its application to nanopositioning. *IEEE T Contr Syst T* 2013; 21(3): 725–738.
6. Esbrook A, Tan X and Khalil H. Inversion-free stabilization and regulation of systems with hysteresis via integral action. *Automatica* 2014; 50(4): 1017–1025.
7. Aljanaideh O, Al Janaideh M and Rakotondrabe M. Enhancement of micro-positioning accuracy of a piezoelectric positioner by suppressing the rate-dependant hysteresis nonlinearities. In: *Proceedings of IEEE/ASME international conference on advanced intelligent mechatronics*, Besançon, 8–11 July 2014, pp.1683–1688. New York: IEEE.
8. Xu Q and Li Y. Dahl model-based hysteresis compensation and precise positioning control of an XY parallel micromanipulator with piezoelectric actuation. *J Dyn Syst: T ASME* 2010; 132(4): 041011-1–041011-12.
9. Gorbet R, Morris K and Wang D. Passivity-based stability and control of hysteresis in smart actuators. *IEEE T Contr Syst T* 2001; 9(1): 5–16.
10. Cruz-Hernandez J and Hayward V. Phase control approach to hysteresis reduction. *IEEE T Contr Syst T* 2001; 9(1): 17–26.
11. Al Janaideh M, Naldi R, Marconi L, et al. A hybrid system for a class of hysteresis nonlinearity: modeling and compensation. In: *Proceedings of decision and control conference*, Maui, HI, 10–13 December 2012, pp. 5380–5385. New York: IEEE.
12. Jayawardhana B, Logemann H and Ryan EP. PID control of second-order systems with hysteresis. *Int J Control* 2008; 81(8): 1331–1342.
13. Riccardi L, Naso D, Turchiano B, et al. Design of linear feedback controllers for dynamic systems with hysteresis. *IEEE T Contr Syst T* 2014; 22: 1268–1280.
14. Francis B and Wonham W. The internal model principle of control theory. *J Appl Math Optim* 1975; 12(5): 170–194.
15. Al Janaideh M and Krejci P. Inverse rate-dependent Prandtl-Ishlinskii model for feedforward compensation of hysteresis in a piezomicropositioning actuator. *IEEE/ASME T Mech* 2013; 18(5): 1498–1507.
16. Wonham W. *Linear multivariable control: a geometric approach*. New York: Springer-Verlag, 1979.
17. Davison EJ. The robust control of a servomechanism problem for linear time-invariant multivariable systems. *IEEE T Automat Contr* 1976; 21(1): 25–34.
18. Astrom KJ and Hagglund T. *Advanced PID control*. Research Triangle Park, NC: The Instrumentation, Systems, and Automation Society, 2006.
19. Yan J, D’Amato AM, Sumer D, et al. Adaptive control of uncertain Hammerstein systems using auxiliary nonlinearities. In: *Proceedings of decision and control conference*, Maui, HI, 10–13 December 2012, pp.4811–4816. New York: IEEE.
20. Al Janaideh M and Bernstein DS. Inversion-free adaptive control of uncertain systems with shape-memory-alloy actuation. In: *Proceedings of American control conference*, Washington, DC, 17–19 June 2013, pp. 3585–3590. New York: IEEE.
21. Al Janaideh M, Yan J, D’Amato AM, et al. Retrospective-cost adaptive control of uncertain Hammerstein-Wiener systems with memoryless and hysteretic nonlinearities. In: *AIAA guidance, navigation and control conference*, Minneapolis, MN, 13–16 August 2012, paper no. AIAA-2012-4449-671. Reston, VA: AIAA.
22. Venugopal R and Bernstein DS. Adaptive disturbance rejection using ARMARKOV system representations. *IEEE T Contr Syst T* 2000; 8(2): 257–269.
23. Hoagg JB, Santillo MA and Bernstein DS. Discrete-time adaptive command following and disturbance rejection for minimum-phase systems with unknown exogenous dynamics. *IEEE T Automat Contr* 2008; 53(4): 912–928.
24. Santillo MA and Bernstein DS. Adaptive control based on retrospective cost optimization. *J Guid Contr Dynam* 2010; 33(2): 289–304.
25. Fledderjohn M, Holzel M, Palanhandalam-Madapusi H, et al. A comparison of least squares algorithms for estimating Markov parameters. In: *Proceedings of American control conference*, Baltimore, MD, 30 June–2 July 2010, pp. 3735–3740. New York: IEEE.
26. Slotine J and Li W. *Applied nonlinear control*. Englewood Cliffs, NJ: Prentice Hall, 1991.
27. Shan Y and Leang K. Design and control for high-speed nanopositioning: serial-kinematic nanopositioners and repetitive control for nanofabrication. *IEEE Contr Syst Mag* 2013; 33(6): 86–105.